Oscillator strengths for N II lines, including intersystem lines, and tests of the spectroscopic coupling scheme

J. Musielok,* J. M. Bridges, S. Djurović,† and W. L. Wiese
National Institute of Standards and Technology, Gaithersburg, Maryland 20899

(Received 5 October 1995; revised manuscript received 25 January 1996)

We have measured the relative line strengths for a fairly large number of lines of the $3s$-$3p$ and $3p$-$3d$ transition arrays of N II with a wall-stabilized arc source in order to test the quality of recent advanced atomic structure calculations. We have observed significant deviations from LS coupling for weaker $3p$-$3d$ lines and have found that our measurements agree much better with recent intermediate coupling results. Also, fairly strong intersystem, or spin-forbidden, lines occur for the N II ion due to a near coincidence of the $3s\ ^1P^o$ and $3s\ ^3P^o$ levels. We provide experimental comparison data for two recent calculations that differ by a factor of 2 for these intersystem lines.

PACS number(s): 32.70.Cs, 32.90.+a

I. INTRODUCTION

Accurate oscillator strengths for the spectral lines of the common gases are required for spectroscopic studies of laboratory and astrophysical plasmas. Recently, an advanced atomic structure calculation [1] has provided such radiation data for N II on a very large scale. This calculation, which is part of the Opacity Project, an international collaboration of about 20 atomic structure theorists in the late 1980s, is based on the close-coupling approximation, which was applied in conjunction with the R-matrix method and has yielded roughly 10^3 *multiplet* values for N II. The critical problem of how to account for the mutual interaction between the atomic electrons—the electron correlation problem—has been taken care of with an extensive configuration-interaction treatment. However, this method can be extended to individual spectral lines only by making use of LS-coupling line strength fractions. Another advanced calculational approach, an extensive configuration-interaction calculation with the CIV3 code [2], has been carried out on a less comprehensive scale, but all the way to individual line strengths. This approach does not assume LS coupling, but includes relativistic corrections of the Breit-Pauli type so that the line strengths are obtained in intermediate coupling (IC).

Significant differences between the results of the two methods are encountered, which reach factors of two for some multiplets and lines. Because numerous approximations are involved, such advanced calculations still cannot provide rigorous estimates of the uncertainties encountered. One may, however, obtain reliable uncertainty estimates from experimental results. Thus, some accurate experimental data are required (a) to establish with confidence the uncertainties of advanced calculations and (b) to settle especially the question to what degree LS coupling is applicable for the individual line strengths in this spectrum. This study was undertaken to provide such experimental comparison data since they do not exist as yet (the only available early emission experiment [3] suffers from significant inaccuracies inherent in photographic data acquisition).

Also, some fairly strong intersystem, or spin-forbidden, lines occur for N II because of a near coincidence of the $3s\ ^1P^o$ and $3s\ ^3P^o$ levels. Two recent calculations [2,4] have produced results for these lines that differ systematically by a factor of 2. We provide experimental comparison data.

II. EXPERIMENTAL PART

We have generated the spectrum of singly ionized nitrogen in a wall-stabilized arc discharge, a source that has been previously described in detail [5,6]. This source produces a cylindrical plasma with a length of about 50 mm and a diameter of 4 mm. The plasma is confined within a channel formed by a stack of seven insulated water-cooled copper disks, which have a central bore of 4 mm. The arc operates between a water-cooled tungsten cathode and a water-cooled copper anode. The electrode areas are also fully enclosed and are purged with argon. The midsection of the arc, which is used for side-on observations, is operated in helium with a small admixture of nitrogen. The nitrogen admixture is carefully controlled with gas-flow meters. Also, the intensity of a strong N II line is continuously monitored during the runs with a 0.25-m spectrometer. Short-term fluctuations as well as long term drift have been held within $\pm 1\%$.

With the operation of the arc discharge in helium as carrier gas we have achieved significant ionization of nitrogen at a moderate arc current of 50 A and at the same time obtained sufficient excitation of the N II lines for accurate intensity measurements. These conditions are realized because helium has such high excitation and ionization energies that in plasmas of partial local thermodynamic equilibrium (partial LTE), such as ours [5], the small nitrogen admixture, with its much smaller ionization and excitation energies, is ionized and excited first. In addition, the use of helium as a carrier gas makes it possible to keep the density of free electrons relatively low, so that Stark broadening is insignificant, resulting in narrow line shapes and readily resolved component lines within multiplets. Also, the ratios of line-to-continuum intensities are quite large since the low electron density suppresses the continuum radiation.

*Permanent address: Opole University, 45-052 Opole, Poland.
†Permanent address: University of Novi Sad, Yugoslavia.

TABLE I. Comparison of calculated and measured relative line strengths in multiplets of single ionized nitrogen (see also Figs. 1 and 2). The line strengths are normalized to multiplet sums of 100.

		Wavelength	Experiment		Theory		
Multiplet	J_1-J_u	(Å)	This work	Ref. [3]	LS	Ref. [2]	Ref. [4]
			$3s$-$3p$ transitions				
$^3P^o$-^3D	2-3	5679.56	48.5 ± 1.4	50.5	46.7	47.4	48.3
	1-2	5666.63	23.4 ± 0.7	24.2	25.0	24.6	23.8
	0-1	5676.02	11.5 ± 0.3	10.6	11.1	11.5	11.6
	2-2	5710.77	8.32 ± 0.25	6.96	8.33	8.16	8.29
	1-1	5686.21	7.68 ± 0.23	7.73	8.33	7.81	7.42
	2-1	5730.66	0.63 ± 0.03		0.56	0.53	0.54
$^3P^o$-^3P	2-2	4630.54	42.7 ± 1.2	43.7	41.7	42.8	43.4
	1-1	4613.87	7.67 ± 0.23	6.04	8.33	7.62	7.35
	2-1	4643.09	14.8 ± 0.4	17.2	13.9	15.1	15.3
	1-0	4621.39	10.7 ± 0.3	9.02	11.1	10.8	10.4
	1-2	4601.48	13.0 ± 0.4	13.5	13.9	13.1	12.6
	0-1	4607.15	11.2 ± 0.3	10.7	11.1	10.7	10.9
$^3P^o$-^3S	2-1	5045.10	52.2 ± 1.4	54.6	55.6	53.1	53.8
	1-1	5010.62	34.3 ± 1.0	34.6	33.3	34.2	32.8
	0-1	5002.70	13.4 ± 0.4	10.8	11.1	12.7	13.4
			$3p$-$3d$ transitions				
^3D-$^3F^o$	3-4	5005.15	43.3 ± 1.7	43.7	42.9	43.0	
	2-3	5001.47	29.9 ± 1.7	29.8	29.6	30.2	
	1-2	5001.13	20.0 ± 1.2	20.1	20.0	20.2	
	3-3	5025.66	3.09 ± 0.12	3.06	3.70	3.14	
	2-2	5016.38	3.48 ± 0.68	3.28	3.70	3.37	
	3-2	5040.71	<0.2		0.10	0.08	
^3D-$^3D^o$	3-3	4803.29	45.7 ± 1.1	45.6	41.4	44.7	
	2-2	4788.14	24.2 ± 0.6	25.6	23.2	25.0	
	1-1	4779.72	13.2 ± 0.3	15.5	15.0	14.9	
	3-2	4810.30	5.22 ± 0.16	4.51	5.20	4.79	
	2-1	4793.65	4.79 ± 0.14	5.06	5.00	4.65	
	2-3	4781.19	3.27 ± 0.16		5.20	2.84	
	1-2	4774.24	3.63 ± 0.11	3.65	5.00	3.18	
^3S-$^3P^o$	1-2	5007.33	56.3 ± 1.6	57.8	55.6	56.9	
	1-1	4994.37	33.0 ± 1.0	33.0	33.3	32.5	
	1-0	4987.38	10.7 ± 0.5	9.25	11.1	10.6	
^3P-$^3D^o$	2-3	5941.65	47.2 ± 1.4	49.7	46.7	46.7	
	1-2	5931.78	25.6 ± 0.7	24.4	25.0	25.5	
	0-1	5927.81	12.1 ± 0.3	11.4	11.1	11.5	
	2-2	5952.39	7.26 ± 0.21	7.50	8.33	7.69	
	1-1	5940.24	7.21 ± 0.21	6.96	8.33	8.14	
	2-1	5960.91	0.55 ± 0.20		0.56	0.49	
^3P-$^3P^o$	2-2	5495.65	44.8 ± 1.3		41.7	44.4	
	1-1	5462.58	11.1 ± 0.3		8.33	10.9	
	2-1	5480.05	13.5 ± 0.4		13.9	14.3	
	1-0	5454.22	11.9 ± 0.3		11.1	12.1	
	1-2	5478.09	9.29 ± 0.28		13.9	8.72	
	0-1	5452.07	9.35 ± 0.28		11.1	9.67	

As in our recent N I emission work [5], we carried out the side-on observations at the position of the central arc disk. This special disk has a small hole in its wall for side-on viewing at a position of full plasma constriction. The spectroscopic measurements were carried out with a 2-m Czerny-Turner scanning monochromator that was equipped with a grating of 1800 groves/mm blazed at 5000 Å. As a radiance standard, we used a tungsten strip lamp calibrated by the Radiometric Physics Division at the National Institute of Standards and Technology (NIST) for all lines except for the intersystem lines at 2139 and 2143 Å. For these lines a NIST calibrated argon mini-arc radiance standard was used. The radiation from either the helium-nitrogen arc or the radiance standards, which were located at the same distance and utilized the same optical system via a rotating mirror, was imaged (with a slight magnification) on the entrance slit of the monochromator. The detection of all radiances was done with photomultipliers having S-1 or S-5 photocathodes.

All aspects of the spectral scans, including the rotation of the grating by a stepping motor as well as the data acquisition, were controlled by a computer that was also employed to perform the line intensity analysis. The analysis was carried out by fitting the recorded line shapes to the sum of a Lorentzian and a Gaussian function plus a slowly varying continuum background. Possible asymmetries in the line profiles due to Stark broadening [7] were expected to be very small and were indeed found to be negligible. All line intensity measurements were repeated at least 5 times and were found to be reproducible within $\pm 2\%$ on an absolute scale.

III. PLASMA DIAGNOSTICS

We operated the wall-stabilized arc at about the same discharge conditions as in our earlier work on N I [5], i.e., at the same current and at atmospheric pressure and with nearly the same He-N_2 gas mixture. Our diagnostic measurements for the present experiment were based on the same techniques as before. We obtained similar values for the excitation, or electron, temperature, i.e., $T_{exc} = 14\,180$ K and for the electron density, $N_e = 2\times10^{15}$ cm^{-3}. However, the requirements for the determination of the temperature and electron density are much less critical in this experiment than in the earlier one, since we compare the relative strengths of lines within the $3s$-$3p$ and $3p$-$3d$ multiplets as two separate entities. In each set the upper levels of the lines differ only slightly in energy, or are in some cases identical, resulting in the intensity ratios of such lines to be only slightly temperature dependent. The electron density is, as in our earlier arc experiment, much larger than that required to ensure partial LTE among the upper levels of the various N II multiplets investigated by us [6].

Another important requirement for the line intensity measurements is the condition that the emission originates from an optically thin layer at every wavelength. Using an earlier described technique [8] involving the doubling of the optical path length and the use of intensity ratio measurements between double and single paths, we found that all investigated lines are indeed emitted from an optically thin layer.

IV. RESULTS AND DISCUSSION

Our main objective has been to measure the oscillator strengths of numerous N II lines to provide accurate experimental comparison data for the recent comprehensive calculations of multiplet and line oscillator strengths. We also wanted to examine to what degree *LS* coupling is approached for the line strengths in multiplets. We have measured the relative oscillator strengths of all lines in the three multiplets comprising the $3s$-$3p$ transition array and five multiplets of the $3p$-$3d$ transition array. Our results, together with the *LS* coupling and the calculated intermediate coupling data, are shown in Table I. All line strengths are normalized to multiplet sums of 100. For the line strengths of the $3s$-$3p$ transition array our measurements as well as the intermediate coupling calculations by Bell, Hibbert, and Stafford [2] and by Weiss [4] are in good agreement with the

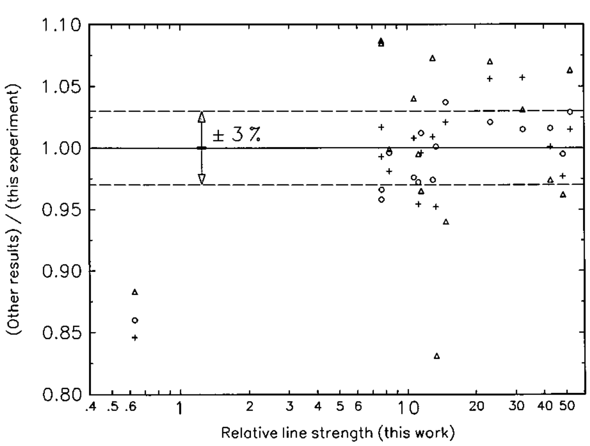

FIG. 1. Comparison of our measured line strengths, normalized within each multiplet to 100, with line strengths according to *LS* coupling (triangles) and the intermediate coupling data of Ref. [2] (pluses) and Ref. [4] (circles) for lines within $3s$-$3p$ triplets. We show an error band of $\pm 3\%$ (broken lines), since our experimental uncertainties lie in the range from $\pm 2.6\%$ to $\pm 3\%$ for all but the weakest line (where the uncertainty is $\pm 5\%$).

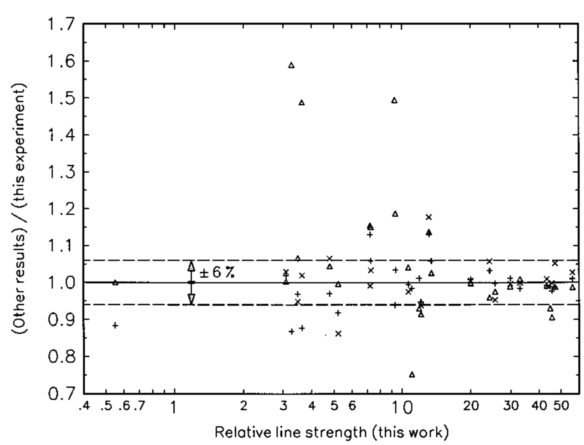

FIG. 2. Comparison of our measured line strengths, normalized within each multiplet to 100, with line strengths according to *LS* coupling (triangles), the intermediate coupling data of Ref. [2] (pluses), and the measurements of Ref. [3] (crosses) for lines within $3p$-$3d$ triplets. The broken lines indicate an error band of $\pm 6\%$, since—with only two exceptions—our experimental uncertainties lie in the range from $\pm 2.5\%$ to $\pm 6\%$.

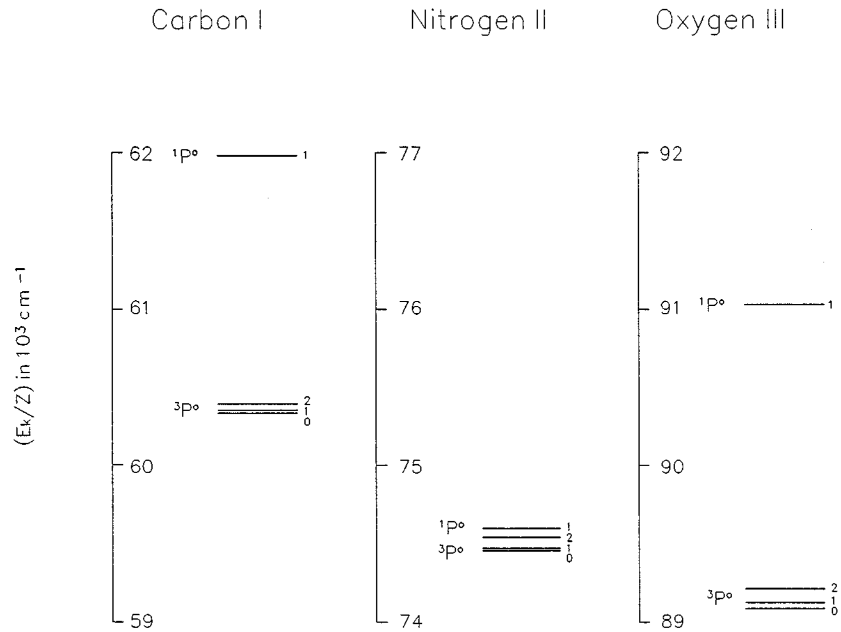

FIG. 3. Partial energy level diagrams for the isoelectronic species C I, N II, and O III, showing the location of the 3s $^1P_1^o$ and 3s $^3P_{0,1,2}^o$ levels. The excitation energy (E_k) for each species is divided by the corresponding value of Z, the effective nuclear charge seen by the valence electron ($Z=1$ for C I, $Z=2$ for N II, and $Z=3$ for O III).

LS-coupling data. Significant deviations from LS coupling occur only for the weakest line in the 3s $^3P^o$–3p ^3S multiplet, both for our experiment and the two IC calculations. An earlier experimental emission result, obtained by Mastrup and Wiese [3] with a similar wall-stabilized arc, but based on the less accurate photographic data acquisition technique, does not show this deviation from LS coupling. For weak lines of the 3p-3d multiplets, the intermediate coupling calculations of Bell, Hibbert, and Stafford [2], as well as our experiment and the earlier arc emission work [3] all deviate significantly from the LS-coupling values.

The LS-coupling branching fractions, the results of the intermediate coupling calculations, and the earlier emission data are also compared graphically with our results in Figs. 1 and 2. Figure 1 indicates that both the LS-coupling data and intermediate coupling calculations agree closely with our results for the lines of the 3s-3p multiplets, except for a few weak lines, as noted above. However, it is also apparent that the agreement of our data with the IC results of Refs. [2] and [4] is better than with the LS-coupling calculations. The only exception is the weakest line of the 3s $^3P^o$-3p ^3D multiplet at 5730.66 Å where the IC calculations yield somewhat larger deviations from our result than the LS-coupling data. For the line strengths of the 3p-3d transition array, presented in Fig. 2, our results show larger departures from LS coupling for some weaker lines. On the other hand, the agreement with the IC calculations and the earlier emission data [3] is quite good.

Another objective of this experiment was to test the accuracy of the line strength data for intersystem lines, which were recently calculated by Bell, Hibbert, and Stafford [2] and Weiss [4]. The spectrum of N II exhibits a number of relatively strong intersystem lines, which are an unusual feature in the spectra of light atoms and ions. In pure LS coupling, intersystem lines are forbidden, and in situations close to LS coupling these lines are normally very weak, having strengths $\leqslant 10^{-2}$ of LS-allowed lines. However, in N II some intersystem lines have strengths that are comparable to or are even larger than those of prominent LS-allowed lines. This special situation arises from a near coincidence of the 3s $^1P^o$ and 3s $^3P^o$ levels, which occurs for the N II ion but not for the neighboring isoelectronic species C I and O III, as shown in Fig. 3.

Accurate calculations of line strengths are more difficult for spin-forbidden or intersystem lines than for the prominent LS multiplets. Indeed, large differences between experiment and theory exist for the strengths of intersystem lines in some light neutral atoms [4,9,10]. We have thus measured a number of intersystem lines in the visible and near UV spectrum, and we have compared our measured line strength ratios:

$$\frac{S(\text{intersystem line})}{S(LS\text{-allowed line})},$$

with the ratios calculated by Weiss [4] and Bell, Hibbert, and Stafford [2], for line pairs with the same upper levels (Table II). One observes very good agreement with the values of Ref. [4], but systematic differences with the results of Ref. [2] insofar as all of the calculated intersystem lines appear to be too weak.

In Table III, we present all our measured line data on an absolute basis. We normalized the strength of the $^3P^o$-^3S multiplet of the 3s-3p transition array to the average of the two recent calculations of Bell, Hibbert, and Stafford [2] and Weiss [4] and have put all lines of the 3s-3p array on this scale, utilizing measured intensity ratios between lines of different multiplets and the arc excitation temperature. Likewise, we have normalized the strength of the ^3S-$^3P^o$ multiplet of the 3p-3d array to Refs. [1] and [2] and have put all 3p-3d lines on this scale. Finally, we have normalized the 3s $^3P^o$–3p ^1S, ^1P,^1D triplet-singlet intersystem lines to the respective 3s $^1P^o$–3p ^1S,^1P,^1D singlets, using again the theoretical data cited above [1,2,4] as the reference for the singlets.

Our normalization procedures minimize experimental uncertainties, since the temperature dependence of our data is nonexistent for some lines and very small for all others, and

TABLE II. Ratios of line strengths between intersystem and LS-allowed lines of the $3s$-$3p$ transition array originating from the same upper levels.

Level		Wavelength	$S_{\text{intersystem}}/S_{\text{allowed}}$			Ratio (theory)/(this expt.)	
			This	Theory			
Lower	Upper	(Å)	Experiment	Ref. [4]	Ref. [2]	(Ref. [4])/(expt.)	(Ref. [2])/(expt.)
$^1P_1^o$	$^3S_1$	*5073.59*	*intersystem line*				
$^3P_0^o$	$^3S_1$	5002.70	0.318 ± 0.031	0.306	0.160	0.96	0.50
$^3P_1^o$	$^3S_1$	5010.62	0.125 ± 0.010	0.121	0.060	0.97	0.48
$^3P_2^o$	$^3S_1$	5045.10	0.081 ± 0.008	0.0738	0.038	0.91	0.47
$^1P_1^o$	$^3P_2$	*4654.53*	*intersystem line*				
$^3P_1^o$	$^3P_2$	4601.48	0.100 ± 0.009	0.0917	0.0405	0.92	0.41
$^3P_2^o$	$^3P_2$	4630.54	0.0313 ± 0.0030	0.0267	0.0124	0.85	0.40
$^1P_1^o$	$^3P_1$	*4667.21*	*intersystem line*				
$^3P_0^o$	$^3P_1$	4607.15	0.093 ± 0.009	0.0758	0.0391	0.82	0.42
$^3P_1^o$	$^3P_1$	4613.87	0.135 ± 0.010	0.112	0.0546	0.83	0.49
$^3P_2^o$	$^3P_1$	4643.09	0.0696 ± 0.0070	0.0534	0.0276	0.77	0.40
$^1P_1^o$	$^3P_0$	*4674.91*	*intersystem line*				
$^3P_1^o$	$^3P_0$	4621.39	0.108 ± 0.010	0.0989	0.0457	0.92	0.42
$^1P_1^o$	$^3D_2$	*5747.30*	*intersystem line*				
$^3P_1^o$	$^3D_2$	5666.63	0.105 ± 0.010	0.0990	0.0460	0.94	0.44
$^3P_2^o$	$^3D_2$	5710.77	0.298 ± 0.030	0.294	0.0139	0.99	0.47
$^1P_1^o$	$^3D_1$	*5767.45*	*intersystem line*				
$^3P_0^o$	$^3D_1$	5676.02	0.089 ± 0.008	0.0913	0.0485	1.02	0.55
$^3P_1^o$	$^3D_1$	5686.21	0.135 ± 0.014	0.143	0.0711	1.06	0.53
$^3P_2^o$	$^3D_1$	5730.66	1.63 ± 0.16	1.96	1.041	1.20	0.64
$^3P_1^o$	$^1S_0$	*3408.13*	*intersystem line*				
$^1P_1^o$	$^1S_0$	3437.14	0.111 ± 0.011	0.0978	0.0451	0.88	0.41
$^3P_1^o$	$^1P_1$	*6379.62*	*intersystem line*				
$^1P_1^o$	$^1P_1$	6482.05	0.190 ± 0.020	0.128	0.0646	0.67	0.34
$^1D_2^o$	$^1P_1$	4895.12	3.23 ± 0.44		1.016		0.32
$^3P_1^o$	$^1D_1$	*3955.85*	*intersystem line*				
$^1P_1^o$	$^1D_1$	3995.00	0.096 ± 0.006	0.0964	0.0444	1.00	0.46

wavelength-dependent errors are small as well. However, we have to consider the uncertainties of the averaged theoretical data [1,2,4], on which all our results are based. These data are estimated to be uncertain by amounts varying from $\pm3\%$ for $3s$-$3p$ triplets to $\pm10\%$ for the $3p$-$3d$ triplets.

Of main interest in Table III are the measured strengths of the intersystem lines which are as reliable as, or better than, the best theoretical data. The listed comparison data are the new NIST tables [11], which are based mostly on the results of Refs. [1,2,4], and the earlier emission data of Mastrup and Wiese [3].

We have also measured the transition probability ratio for two intersystem transitions out of the ground state, $(2s^22p^2\ ^3P_2–2s2p^3\ ^5S_2^o)/(2s^22p^2\ ^3P_1–2s2p^3\ ^5S_2^o)$ at 2143 Å/2139 Å, and obtain a value of 2.24 ± 0.06. This ratio was also calculated by Hibbert and Bates [12] and Froese Fischer and Saha [13]. Their results, 2.22 and 2.48, respectively, are in close agreement with our experimental value and thus allow the existing lifetime data for the $2s2p^3\ ^5S_2^o$ level [14,15] to be reliably distributed between the two component lines.

The uncertainties listed for the transition probabilities in Tables I, II, and III have been estimated by taking into account the same contributing factors as given in our earlier paper [5]. We present ‘‘expanded’’ uncertainties, i.e., twice the standard deviations. The latter are equal to the root of the

TABLE III. Transition probabilities of N II lines (in 10^8 s^{-1}). Our results for all 3s-3p lines are normalized to the multiplet value of 3s $^3P^o$-3p ^3S (part A) and for all 3p-3d lines to the multiplet value of 3p ^3S-3d $^3P^o$ (part B). For the intersystem lines, our results are normalized to the related singlet transitions listed in the table (part C). The absolute values are taken from Ref. [11], which are based on the average of results from Refs. [1,2,4]. For comparison, we present in columns 5 and 6 the data from the new NIST tables [11] and the results of a previous emission experiment [3]. In the last two columns, we give the ratios of the two comparison data sets [3,11] to our results.

Multiplet	Wavelength (Å)	J_1-J_u	Transition probabilities: This work	Transition probabilities: Ref. [11]	Transition probabilities: Ref. [3]	Ratios: NIST/(expt.)	Ratios: (Ref. [3])/(expt.)
			A. 3s-3p transitions				
$^3P^o$-^3D	5679.56	2-3	0.484±0.044	0.525	0.632	1.085	1.306
	5666.63	1-2	0.328±0.030	0.374	0.436	1.140	1.329
	5676.02	0-1	0.268±0.021	0.296	0.314	1.105	1.172
	5710.77	2-2	0.114±0.010	0..124	0.122	1.088	1.070
	5686.21	1-1	0.178±0.016	0.194	0.235	1.090	1.320
	5730.66	2-1	0.0143±0.0017	0.0134		0.937	
$^1P^o$-^3D	5747.30	1-2	0.0332±0.0030	0.0340		1.024	
	5767.45	1-1	0.0229±0.0021	0.0244		1.066	
$^3P^o$-^3S	5045.10	2-1	0.333±0.013	0.342	0.389	1.027	1.169
	5010.62	1-1	0.223±0.011	0.219	0.252	0.982	1.132
	5002.70	0-1	0.0874±0.0048	0.0845	0.0809	0.967	0.926
$^1P^o$-^3S	5073.59	1-1	0.0267±0.0021	0.0259		0.97	
$^3P^o$-^3P	4630.54	2-2	0.886±0.071	0.772	0.898	0.871	1.013
	4613.87	1-1	0.268±0.024	0.226	0.213	0.843	0.795
	4643.09	2-1	0.507±0.041	0.451	0.499	0.890	0.985
	4621.39	1-0	1.11±0.089	0.955	0.965	0.857	0.866
	4601.48	1-2	0.274±0.025	0.235	0.284	0.858	1.035
	4607.15	0-1	0.392±0.31	0.326	0.366	0.832	0.934
$^1P^o$-^3P	4654.53	1-2	0.0272±0.0025	0.0243		0.893	
	4667.21	1-1	0.0348±0.0032	0.0299		0.859	
	4674.91	1-0	0.116±0.010	0.105		0.905	
			B. 3p-3d transitions				
^3D-$^3F^o$	5005.15	3-4	1.29±0.11	1.16	1.27	0.899	0.985
	5001.47	2-3	1.14±0.14	1.05	1.20	0.921	1.055
	5001.13	1-2	1.07±0.13	0.976	1.13	0.912	1.060
	5025.66	3-3	0.117±0.009	0.107	0.123	0.914	1.052
	5016.38	2-2	0.185±0.040	0.162	0.186	0.876	1.006
	5040.71	3-2	<0.009	0.003 78			
^3D-$^3D^o$	4803.29	3-3	0.344±0.027	0.318	0.388	0.924	1.127
	4788.14	2-2	0.258±0.021	0.252	0.277	0.977	1.073
	4779.72	1-1	0.235±0.019	0.252	0.285	1.072	1.211
	4810.30	3-2	0.0548±0.0048	0.475	0.0484	0.867	0.884
	4793.65	2-1	0.0847±0.0076	0.0777	0.0904	0.917	1.067
	4781.19	2-3	0.0250±0.0030	0.0205		0.820	
	4774.24	1-2	0.0390±0.0035	0.0324	0.0410	0.831	1.050
^3S-$^3P^o$	5007.33	1-2	0.782±0.055	0.789	0.904	1.009	1.155
	4994.37	1-1	0.771±0.054	0.760	0.867	0.986	1.125
	4987.38	1-0	0.751±0.083	0.748	0.735	0.996	0.979

TABLE III. (*Continued*).

Multiplet	Wavelength (Å)	J_1-J_u	Transition probabilities: This work	Ref. [11]	Ref. [3]	Ratios: NIST/(expt.)	(Ref. [3])/(expt.)
^3P-$^3D^o$	5941.65	2-3	0.466 ± 0.060	0.554	0.621	1.189	1.332
	5931.78	1-2	0.355 ± 0.042	0.427	0.427	1.203	1.203
	5927.81	0-1	0.282 ± 0.031	0.322	0.334	1.142	1.184
	5952.39	2-2	0.0997 ± 0.0130	0.127	0.129	1.274	1.291
	5940.24	1-1	0.166 ± 0.021	0.226	0.209	1.361	1.262
	5960.91	2-1	0.012 ± 0.004	0.0134		1.117	
^3P-$^3P^o$	5495.65	2-2	0.226 ± 0.018	0.240		1.062	
	5462.58	1-1	0.0946 ± 0.0076	0.100		1.057	
	5480.05	2-1	0.114 ± 0.010	0.130		1.140	
	5454.22	1-0	0.307 ± 0.022	0.334		1.088	
	5478.09	1-2	0.0472 ± 0.0042	0.0475		1.006	
	5452.07	0-1	0.0803 ± 0.0072	0.0889		1.017	
C. $3s$-$3p$ triplet-singlet intersystem lines							
$^1P^o$-^1S	3437.14	1-0		2.07			
$^3P^o$-^1S	3408.13	1-0	0.236 ± 0.033	0.219		0.928	
$^1P^o$-^1P	6482.05	1-1		0.301			
$^1D^o$-^1P	4895.12	2-1		0.0426			
$^3P^o$-^1P	6379.62	1-1	0.0611 ± 0.007	0.0611		1.000	
$^1P^o$-^1D	3995.00	1-2		1.35			
$^3P^o$-^1D	3955.85	1-2	0.133 ± 0.011	0.131		0.985	

sum of the squares of the individual uncertainty contributions.

Our measurements have thus confirmed experimentally that LS coupling is an excellent approximation for the linestrengths of the s-p transitions of N II, but that departures become noticeable for p-d and np-$(n+1)s$ transitions. They also show that intermediate coupling calculations are a considerable improvement, but still have difficulties in determining the intersystem, or spin-forbidden, line strengths. Our results should provide valuable test data for future atomic structure calculations.

ACKNOWLEDGMENT

J.M. was supported in part by the M. Sklodowska-Curie Foundation.

[1] D. Luo and A. K. Pradhan, J. Phys. B **22**, 3377 (1989).

[2] K. L. Bell, A. Hibbert, and R. P. Stafford, Phys. Scr. **52**, 240 (1995).

[3] F. Mastrup and W. Wiese, Z. Astrophys. **44**, 259 (1958).

[4] A. W. Weiss (unpublished).

[5] J. Musielok, W. L. Wiese, and G. Veres, Phys. Rev. A **51**, 3588 (1995).

[6] W. L. Wiese, in *Methods of Experimental Physics*, edited by B. Bederson and W. L. Fite (Academic, New York, 1968), Vol. 7B, pp. 307–353.

[7] H. R. Griem, *Spectral Line Broadening to Plasmas* (Academic, New York, 1974).

[8] V. Helbig, D. E. Kelleher, and W. L. Wiese, Phys. Rev. A **14**, 1082 (1976).

[9] C. Goldbach, M. Martin, and G. Nollez, Astron. Astrophys. **221**, 155 (1989).

[10] C. Goldbach, T. Luedtke, M. Martin, and G. Nollez, Astron. Astrophys. **226**, 605 (1992).

[11] W. L. Wiese, J. Fuhr, and T. M. Deters, *Atomic Transition Probabilities for Carbon, Nitrogen, and Oxygen*, J. Phys. Chem. Ref. Data Monograph No. 7 (AIP, New York, 1995).

[12] A. Hibbert and D. R. Bates, Planet. Space Sci. **29**, 263 (1981).

[13] C. Froese Fischer and H. P. Saha, Phys. Scr. **32**, 181 (1985).

[14] A. G. Calamai and C. E. Johnson, Phys. Rev. A **44**, 218 (1991).

[15] B. C. Johnson, P. L. Smith, and W. H. Parkinson (private communication).